In Situ Measurement of Grain-orientation-dependent Stress during Deformation of Crystallites

Y. D. Wang,[1] X.-L. Wang,[1] A. D. Stoica,[1] J. D. Almer,[2] U. Lienert,[2] D. R. Haeffner,[2] Y. H. Sha[3]
[1]Spallation Neutron Source, Oak Ridge National Laboratory, Oak Ridge, TN, U.S.A.
[2]Advanced Photon Source, Argonne National Laboratory, Argonne, IL, U.S.A.
[3]Department of Materials Science, Northeastern University, Shenyang, China

Introduction

When a polycrystalline material is deformed, not only macrostresses (average stresses over a certain gauge volume) but also microstresses (variation of stress in the length scale of micrometers) are usually produced. The existence of microstresses in single-phase materials is due to the discontinuity of stress from grain to grain, caused by so-called elastic incompatibility — a cause that was realized more than one decade ago [1]. *In situ* measurements related to the evolution of these microstresses provide the basic data needed by models that simulate important processes (e.g., grain orientation evolution during deformation, recrystallization, and phase transformations) in technical and geological materials.

Previous investigations on the interaction of grains during deformation mainly used 3-D plasticity models [2-4] to predict the stress state of individual orientations, and they compared the simulated results to the experimental diffraction strains for those cluster grains with respect to some specified sample and crystal directions. Direct measurements [5-7] using marker trackers are possible for coarse-grained materials, but only strain distributions near the surface can be captured. Recently, microbeam synchrotron x-ray diffraction techniques that use monochromatic or white beams [8, 9] were developed to trace the orientation evolution and resolve the subsurface stress state of individual grains. However, in order to describe the properties of polycrystalline aggregates, it is necessary to collect the stress distribution data for a large number of individual grains with reliable statistics. Despite recent advances in synchrotron techniques, mapping the local strains of individual grains with a fine grain or deformation-induced substructures in the bulk materials remains a challenge, particularly during *in situ* loading.

An alternative experimental method is to collect information on the stress distribution from specific lattice-plane directions with respect to the sample directions (so-called strain pole figures) by using high-energy x-rays or neutrons. Microstresses are produced by elastic and plastic incompatibility of grains having different orientations; thus, they depend on the local grain orientation. Although the strains of individual grains cannot be resolved with this technique, a statistical distribution of strain/stress as a function of grain orientation (stress orientation distribution function [SODF]) can be constructed from the measured strain pole figures with different hkl-planes [10, 11]. We call this kind of stress the grain-orientation-dependent stress. The microstress is resolved in orientation (Euler) space rather than real space. A systematic investigation on the SODF evolution of bcc metals with different primary microstructures and textures during *in situ* loading has been carried out at the APS. Preliminary results are reported on here.

Methods and Materials

The material studied was commercial, Ti-stabilized, interstitial-free (IF) steel with the following composition (in wt%): 0.003 C, 0.15 Mn, 0.01 P, 0.0073 S, 0.0022 N, 0.001 Nb, 0.011 Si, 0.034 Al, 0.084 Ti, and balance Fe. It was first hot-rolled to a thickness of 3.7 mm and then annealed for 5 h at 750°C in nitrogen to relieve the residual stress due to hot-rolling. The annealed sheets were further cold-rolled to a reduction of 70%. Two kinds of microstructures were prepared: one with the primary deformed microstructure and the other with the recovery microstructure, produced by annealing the cold-rolled sample at 500°C for 2 h. Bone-shaped tensile samples with a cross section of 1×1 m^2 were then produced by spark erosion cutting, with the loading direction (LD) oriented along the rolling direction (RD) and transverse direction (TD) for different samples.

Diffraction measurements were performed with a monochromatic high-energy x-ray beam (E = 80 keV), which allowed full penetration through the 1-mm cross sections. The incident beam size was 0.1×0.1 mm^2. Samples were *in situ* uniaxially loaded in a dedicated tensile stage, which was mounted in a four-circle Huber goniometer. During loading, the sample was rotated around the loading direction (this rotation is defined as ω) over 90° at an interval $\Delta\omega = 10°$. A Mar345 imaging plate (345-mm area, pixel resolution of 150 µm) recorded several Debye rings, simultaneously, at each stage of deformation. The intensity distributions from these rings provide information on grain orientation, while the radial position (2θ) provides strain information. Images were converted to the polar coordinates (radius and azimuth) by using FIT2D. In order to get accurate strain distributions,

Ce_2O reference powder was attached to the one surface of the measured sample.

Results and Discussion

Here, we demonstrate only one example: the strain distributions and SODF for the annealed sample during *in situ* loading along the RD at an applied stress of 480 MPa. Figure 1 shows the measured {110}, {200}, {211}, and {110} strain pole figures. In spite of similar variations for all {hkl}-planes, the Reuss or Voigt assumptions cannot give satisfactory results. For detailed comparisons among those strain distributions, Fig. 2 gives the measured strains for {110}, {200}, and {211} at ω = 10°. The recalculated strains from using different models — Reuss, Voigt, and SODF — are also given in Fig. 2. Neither the Voigt model nor the Reuss model can completely capture the strain variations for all {hkl} planes, while the SODF model does capture them reasonably well.

Table 1 lists the macrostresses calculated by various models and the microstresses for main texture components calculated by the SODF model. It is clear that large microstresses, which depend on the grain orientation, exist. If these microstresses are neglected, the macrostresses cannot be accurately calculated. For example, if either the Reuss model or the Voigt model is used, overestimations for σ_{11}, σ_{22}, or σ_{33} are made.

It can be seen from the microstresses listed in Table 1 that the stress along loading direction (σ_{11}) for the {hkl}<110> texture component is significantly lower than that in {111}<112>. Table 2 lists the Taylor factors (classic Taylor strain model is assumed, along with an elastic modulus of E = 219 GPa) for those orientations (E = 219 GPa). The Taylor factor for the {hkl}<110> orientation is larger than that for {111}<112>. From these Taylor factors, we can estimate the critical shear stress (CRSS) for all texture components (also in Table 2). The CRSS is seen to strongly depend on grain orientation. A

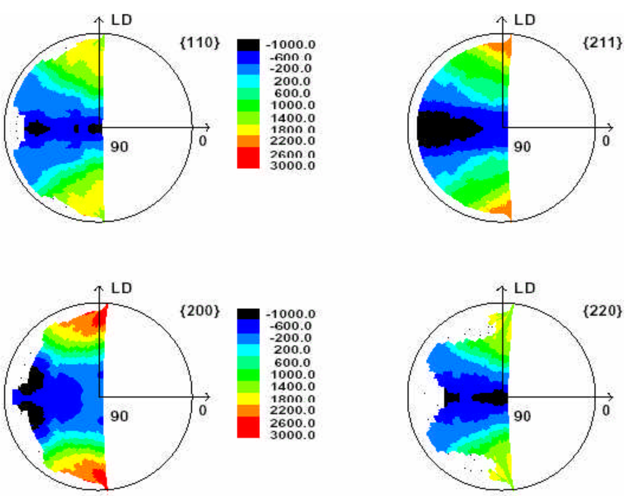

Fig. 1. The measured strain pole figures for annealed IF steel during in situ loading along RD at a stress of 480 MPa.

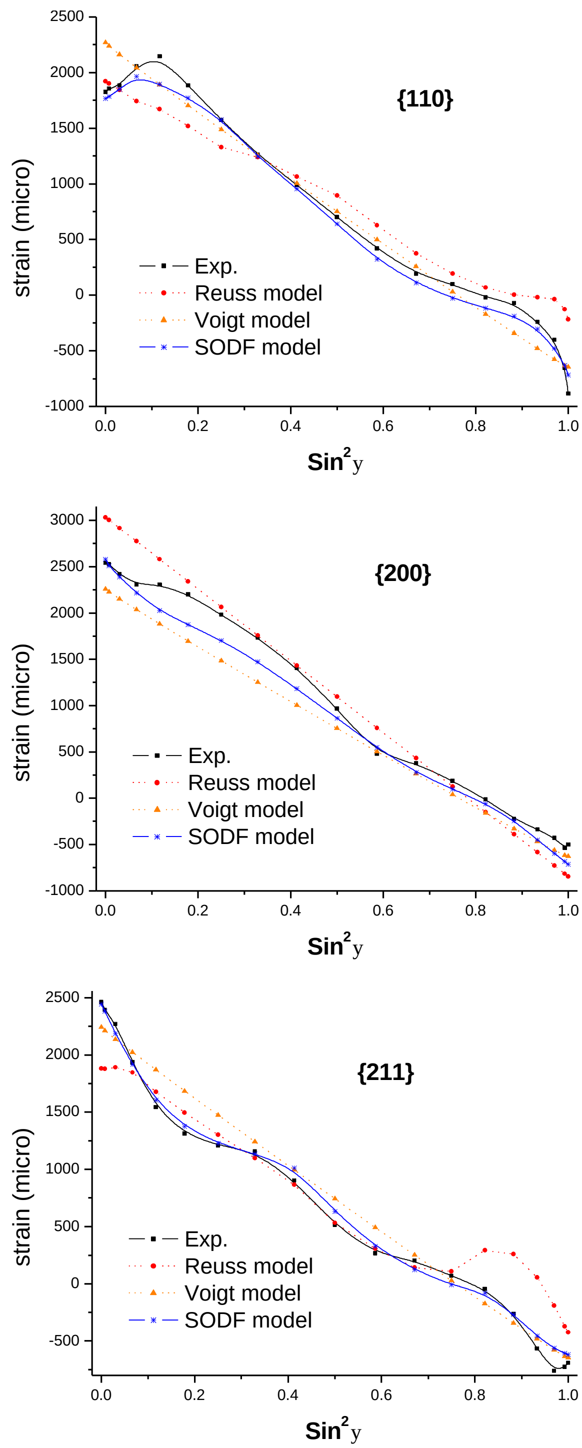

FIG. 2. Measured strain distributions for three diffraction rings and fits to different micromechanical models.

Table 1. Macrostresses calculated by the Reuss, Voigt, and SODF models, and microstresses (in MPa) for main texture components calculated by the SODF model.

Texture component	Euler angle {ψ, θ, φ} (°)	σ_{11}	σ_{22}	σ_{33}	σ_{23}	σ_{13}	σ_{12}
{100}<110>	90, 0, 45	337	-286	-63	0	0	0
{311}<110>	90, 25, 45	373	-167	-55	±60	0	0
{211}<110>	90, 30, 45	396	-224	-49	±67	0	0
{111}<110>	90, 54.7, 45	478	54	-83	±76	0	0
{111}<112>	0, 54.7, 45	676	150	27	0	±50	0
Macrostress	SODF	470	-26	-14	0	0	0
Macrostress	Reuss	491	122	114	-4	-10	-23
Macrostress	Voigt	561	30	40	-11	-8	-7

Table 2. Plasticity information for texture components.

Texture component	Euler angle {ψ, θ, φ} (°)	Taylor factor	CRSS (MPa)
{100}<110>	90, 0, 45	3.62	93
{311}<110>	90, 25, 45	3.62	103
{211}<110>	90, 30, 45	3.62	109
{111}<110>	90, 54.7, 45	3.62	132
{111}<112>	0, 54.7, 45	2.82	240

possible explanation for the anisotropy of CRSS could be connected to the characterizations of microstructures for the studied materials (i.e., the grain-scale heterogeneity during the cold-rolling process). According to electron backscatter pattern (EBSP) observations, during cold-rolling, grains near {111}<uvw> become harder than those near {hkl}<110> [12].

Although the studied sample is annealed at 500°C for 2 h before *in situ* loading, the fine substructures for grains near {111}<uvw> still remain according to the observed microstructures. The formulation of the anisotropic CRSS observed in the IF steel occurs during deformation of crystals, which should be attributed to the presence of dislocation boundaries, which affect the slip behaviors [13]. We provide direct evidence for this argument from the measurements of grain-orientation-dependent stress by using high-energy x-rays.

Detailed results on the evolution of SODF as a function of loading will be reported soon. It should be pointed out that, from the SODFs, rich information can be obtained on the influence of microstructures on the micro-hardening parameters and the real boundary conditions of plastic deformation in a polycrystalline material. These experimental results should be introduced into future crystal plastic deformation simulations to overcome the overpredictions of main texture components made by the present texture models.

Acknowledgments

Use of the APS was supported by the U.S. Department of Energy, Office of Science, Office of Basic Energy Sciences, under Contract No. W-31-109-ENG-38.

References

[1] I. C. Noyan and J. B. Cohen, *Residual Stress — Measurement by Diffraction and Interpretation* (Springer-Verlag, New York, NY, 1987).

[2] P. Dawson, D. Boyce, S. MacEven, and R. Rogge, “Residual strain in HY100 polycrystals: Comparisons of experiments and simulations,” Metall. Trans. A **31**, 1543-1555 (2000).

[3] B. Clausen, T. Lorentz, and T. Leffers, “Self-consistent modeling of the plastic deformation of fcc polycrystals and its implications for diffraction measurements of internal stresses,” Acta Mater. **46**, 3087-3098 (1998).

[4] J. W. L. Pang, T. M. Holden, and T. E. Mason, “*In situ* generation of intergranular strains in an Al7050 alloy,” Acta Mater. **46**, 1503-1518 (1998).

[5] D. Rabbe, M. Sachtleber, Z. Zhao, F. Roters, and S. Zaefferer, “Micromechanical and macromechanical effects in grain scale polycrystal plasticity experimental and simulation,” Acta Mater. **49**, 3433-3441 (2001).

[6] E. E. Nugent, R. B. Calhoun, and A. Mortensen, “Experimental investigation of stress and strain fields in a ductile matrix surrounding an elastic inclusion,” Acta Mater. **48**, 1451-1467 (2000).

[7] F. Delaire, J. L. Raphanel, and C. Rey, “Plastic heterogeneities of a copper multicrystal deformed in uniaxial tension: Experimental study and finite element simulations,” Acta Mater. **48**, 1075-1087 (2000).

[8] L. Margulies, G. Winther, and H. F. Poulsen, “*In situ* measurement of grain rotation during deformation of polycrystals,” Science **291**, 2392-2394 (2001).

[9] B. C. Larson, W. Yang, G. E. Ice, J. D. Budai, and J. Z. Tischler, Nature **415**, 887-890 (2002).

[10] Y. D. Wang, R. L. Peng, and R. L McGreevy, “A novel method for constructing the mean field of grain-orientation-dependent residual stress,” Phil. Mag. Lett. **81**, 153 –163 (2001).

[11] Y. D. Wang, R. L. Peng., X.-L. Wang, and R. L. McGreevy, “Grain-orientation-dependent residual stress and the effect of annealing in cold-rolled stainless steel,” Acta Mater. **50**, 1717-1734 (2002).

[12] B. Hutchinson, “Deformation microstructures and textures in steels,” Phil. Trans. R. Soc. Lond. **357**, 1471-1485 (1999).

[13] N. Hansen and D. J. Jensen, “Development of microstructure in FCC metals during cold work,” Phil. Trans. R. Soc. Lond. **357**, 1447-1469 (1999).